Original Paper

Load dependence of the hardness of silicate glasses – Not just due to indenter tip defects

Peter Grau, Gunnar Berg and Wolfgang Fränzel

Fachbereich Physik, Martin-Luther-Universität Halle-Wittenberg, Halle (Germany)

Martin Schinker

Fraunhofer-Institut für Werkstoffmechanik, Freiburg (Germany)

The real contact area of Berkovich indenters with typical indenter tip defects is calculated as a function of the penetration depth in a general form and compared with literature results for Vickers indenters. The influence of the tip defects on the load dependence of hardness is treated for both types of indenters, taking into account possible purely elastic deformation at the beginning of contact. Using the example of recording microhardness measurements on glass made using a Berkovich indenter, it is shown that a linear dependence exists between load and depth of penetration in the millinewton load region which can be explained by a rounded indenter tip. However, the resulting corrections for the real contact area are not sufficient to compensate for the load dependence of the hardness in the entire load region. A method is proposed for showing definitely that the load dependence of the hardness is caused not just by indenter tip defects but also by material properties. This method is tested on extensive measurements of the authors, as well as on results of Frischat and the Oak Ridge group.

Lastabhängigkeit der Härte von Silicatgläsern – Nicht nur durch Indenterspitzenfehler verursacht

Für die typischen Indenterspitzenfehler wird die reale Kontaktfläche von Berkovich-Indentern als Funktion der Eindringtiefe in einer allgemeinen Form berechnet und mit den Literaturergebnissen für Vickers-Indenter verglichen. Der Einfluß der Spitzenfehler auf die Lastabhängigkeit der Härte wird für beide Indentertypen behandelt, wobei mögliche rein elastische Verformungen zu Kontaktbeginn berücksichtigt werden. Am Beispiel von registrierenden Härtemessungen an Glas mit dem Berkovich-Indenter wird gezeigt, daß im Millinewton-Lastbereich zwischen Last und Eindringtiefe eine lineare Abhängigkeit besteht, die durch eine abgerundete Indenterspitze erklärt werden kann. Die daraus resultierenden Korrekturen für die reale Kontaktfläche reichen aber nicht aus, um die gemessene Lastabhängigkeit der Härte im gesamten Lastbereich zu kompensieren. Es wird ein Verfahren vorgeschlagen, mit dem eindeutig entschieden werden kann, daß die Lastabhängigkeit der Härte nicht allein durch Indenterspitzenfehler, sondern wesentlich durch die Eigenschaften des Materials verursacht wird. Das Verfahren wird an umfangreichen Meßergebnissen der eigenen Gruppe, von Frischat und von der Oak Ridge-Gruppe erprobt.

1. Introduction

Vickers, Knoop and Berkovich hardness testing is associated with a load dependence of hardness, an effect which is most pronounced at the smallest loads [1 and 2]. The reasons for this are still in dispute.

This peculiarity is of particular interest if it is due to the deformation behavior of the material during point loading. This interpretation is in contradiction to Kick's law [3]. Before this explanation can be accepted, the contribution of the experimental conditions must be investigated and isolated. The aim of this paper is to investigate the influence of imperfect indenter tips on the load dependence of the hardness in experiments on different glasses. Glass is selected for this investigation, because corrosion of the glass surface has only a minor influence on the hardness of the glass.

In this work, in analogy to [4], it will be assumed that:

a) the determination of the zero point of the load/penetration curve at the moment of contact can be calculated correctly by a nonlinear regression procedure [5], and

b) the influence of the parasitic deformation of the indenter assembly is minimized by sintering the diamond pyramid in hard metal [6].

If these conditions are realized, the main reason for the load dependence of the hardness which is connected with the test conditions is imperfection of the indenter tip. In this case, calculation of the hardness number leads to a fictive value:

$$H_{\mathrm{fic}} = \frac{F}{A_{\mathrm{ideal}}} . \tag{1}$$

To evaluate the correct hardness number $H(s)$, the real contact area A_{real} must be substituted for the contact area A_{ideal} of the perfect indenter tip:

Received April 15, revised manuscript July 26, 1993.

Table 1. Real contact area for Vickers indenter; $A_{real}(s) = 26.43(\alpha_0 + \alpha_1 s + \alpha_2 s^2)$

	α_0	α_1	α_2
regular tip	0	0	1
roof edge	0	$1\,s_0$	1
blunted tip ($s > s_0$)	$0.93\,s_0^2$	$2\,s_0$	1
rounded tip: $R_2 = 6.6\,s_0$ $s_c = 0.481\,s_0$			
$s < s_c$	0	$1.57\,s_0$	0
$s > s_c$	$0.025\,s_0^2$	$1.04\,s_0$	1
rounded tip: $R_1 = 12.7\,s_0$ $s_c = 0.492\,s_0$			
$s < s_c$	0	$3.02\,s_0$	0
$s > s_c$	$0.74\,s_0^2$	$1.01\,s_0$	1
"elliptical" tip		$1.04\,s_0$	1

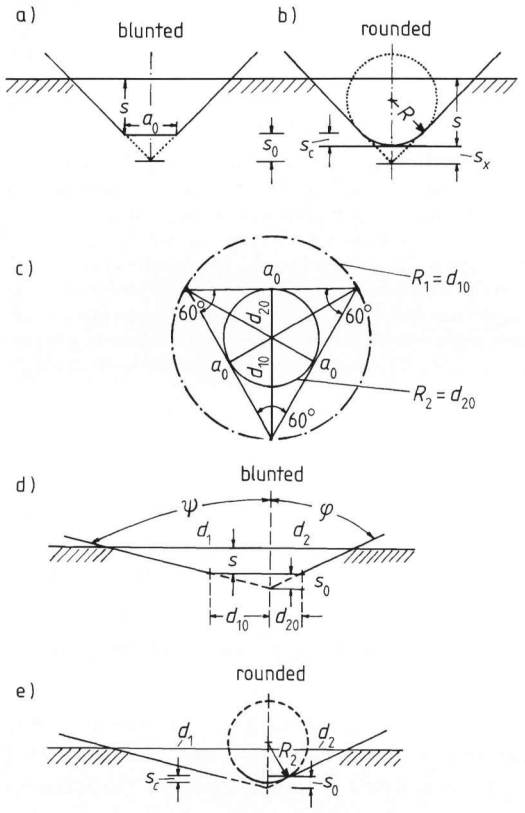

Figures 1a to e. Schematic representations of a blunted (flattened) (figures a and d) and rounded (figures b and e) tip of a Vickers pyramid and a Berkovich tetrahedron, respectively, while figure c shows the cross-section of the indenter in both cases. s = true penetration depth of the damaged indenter, s_0 = defect parameter, s_c = altitude of the ball cap, s_x = missing part of the tip, a_0 = length of the square side (Vickers) or triangle side (Berkovich) of the ground faces of the blunted indenter, R = radius of the ball cap ($R_1 = d_{10}$, i.e., radius of the circumscribing circle, $R_2 = d_{20}$, i.e., radius of the interior circle), d_1, d_2 = parts of the perpendiculars at the midpoints of the sides (d_{10} and d_{20} which are correlated to s_0), φ, ψ = characteristic angles for the Berkovich indenter.

$$H(s) = \frac{F(s)}{A_{real}(s)} . \tag{2}$$

The load $F = F(s)$ is induced by the resistance of the indenter against the penetration into the material, and it can be detected directly only in a closed loop hardness tester.

The contact area, $A_{real}(s)$, of a Vickers impression can be calculated in dependence on the penetration depth for different typical tip defects [4]. The results can be expressed in a general form as a second-degree polynomial:

$$A_{real}(s) = 26.43(\alpha_0 + \alpha_1 s + \alpha_2 s^2) \tag{3}$$

where a_i are geometry parameters which are determined by the defect parameter, s_0, and which are collected in table 1. The definition of s_0 shown in figures 1a to e gives the extent of the defect as the distance between the intact pyramid faces and the extrapolated tip.

With a Berkovich indenter it is possible to realize the point contact condition more exactly than with a Vickers indenter. However, the Berkovich indenter is included in these considerations. The values for the tip angles, $\psi = 77.03°$ and $\varphi = 65.27°$ (see figure 1d), are chosen in such a way that the relation between the contact area and indentation depth, s, is nearly the same for both indenters. The influence of tip defects of a Berkovich indenter on the real contact area, A_{real}, is calculated according to equation (3) in the same manner as for the Vickers indenter, and the results are collected in table 2. The geometrical meanings of the symbols used are explained in figures 1a to e. For the rounded indenter, one must distinguish between the two extreme cases, i.e., that the ball cap touches the indenter faces, or that it touches the sharp indenter edges. For the Berkovich indenter, the first geometric condition leads to the radius of the ball $R_2 = d_{20} = 5.19\,s_0$ with a cap altitude $s_c = 0.476\,s_0$ (see figure 1c), and the second one leads to $R_1 = d_{10} = 19.43\,s_0$ with a cap altitude $s_c = 0.494\,s_0$. For the Vickers indenter, these values are $R_2 = 6.6\,s_0$ with $s_c = 0.481\,s_0$ and $R_1 = 12.7\,s_0$ with $s_c = 0.492\,s_0$, respectively. In both cases, the geometric condition leading to the smaller ball radius, R_2, seems to be the realistic one.

As the next step, a survey of tables 1 and 2 is used to discuss the characteristic influences of the most important indenter defects on the load/penetration curve at the moment of contact.

2. Influence of the tip defects of the indenter on the loading curve

The (analytical) relation between load and penetration depth follows from equation (3) by multiplication with the hardness number, H:

$$F(s) \equiv H_{\text{fic}} \cdot A_{\text{ideal}} \equiv H(s) \cdot A_{\text{real}}(s) ,$$

Vickers: $F(s) = 26.43 \cdot H(s)\,(\alpha_0 + \alpha_1 s + \alpha_2 s^2)$, (4)

Berkovich: $F(s) = 26.98 \cdot H(s)\,(\alpha_0 + \alpha_1 s + \alpha_2 s^2)$.

The following will be discussed under the assumption that the hardness is a constant of the material, i.e., $H(s) = H$ = constant. This means that the load dependence of the hardness is not induced by the properties of the material. In this case, one has the consequences according to [4] and described in sections 2.1 to 2.3.

2.1. Blunted (flattened) indenters, $F < F_0$

The plastic deformation resulting in a permanent impression starts above the critical load $F_0 = HA_0$. Because $A_0 = \alpha_0$ for the ground faces of the blunted indenter, one gets:

Vickers: $F_0 = 26.43\,H \cdot 0.93\,s_0^2 = 24.58\,Hs_0^2$,

Berkovich: $F_0 \equiv 26.98\,H \cdot 0.91\,s_0^2 \equiv 24.55\,Hs_0^2$. (5)

For $F < F_0$, after the first contact the load increases only elastically in proportion to the penetration depth (Timoshenko [7], Pharr et al. [8]):

$$F = m \cdot E_{\text{eff}} A_0^{1/2} s ,$$

Vickers: $F = 5.65\,E_{\text{eff}} s_0 s$, (6)

Berkovich: $F = 5.77\,E_{\text{eff}} s_0 s$.

The geometrical factor, m, is given in [8], and the effective elastic modulus follows from:

$$\frac{1}{E_{\text{eff}}} = \frac{1-\mu_1^2}{E_1} + \frac{1-\mu_2^2}{E_2} . \tag{7}$$

E_i are the Young's moduli of the indenter and the sample, respectively, and μ_i are the corresponding values of Poisson's ratio.

2.2. Rounded indenters, $s < s_c$

The relation between F and s at small penetration depths ($s < s_c$) is also linear for rounded indenter tips, but the deformation process is plastic (represented by the hardness number H = constant) even at the very start of contact. This is shown by the following relations derived from the ball indentation method:

Vickers: $F = 26.43\,H \cdot 1.57\,s_0\,s = 41.5\,Hs_0 s$,

Berkovich: $F \equiv 26.98\,H \cdot 1.21\,s_0\,s \equiv 32.6\,Hs_0 s$. (8)

The critical depth, $s = s_c$, is reached at the critical load F_0:

Table 2. Real contact area for Berkovich indenter; $A_{\text{real}}(s) \equiv 26.977(\alpha_0 + \alpha_1 s + \alpha_2 s^2)$

	α_0	α_1	α_2
regular tip	0	0	1
blunted tip ($s > s_0$)	$0.91\,s_0^2$	$2s_0$	1
rounded tip: $R_2 \equiv 5.19\,s_0$ $s_c \equiv 0.476\,s_0$			
$s < s_c$	0	$1.21\,s_0$	0
$s > s_c$	$-0.15\,s_0^2$	$1.05\,s_0$	1
rounded tip: $R_1 = 19.34\,s_0$ $s_c = 0.494\,s_0$			
$s < s_c$	0	$4.51\,s_0$	0
$s > s_c$	$1.48\,s_0^2$	$1.01\,s_0$	1

Vickers: $F_0 = 26.43\,H \cdot 0.78\,s_0^2 = 20.75\,Hs_0^2$,

Berkovich: $F_0 \equiv 26.98\,H \cdot 0.58\,s_0^2 = 15.52\,Hs_0^2$. (9)

One must add an $s^{3/2}$ term to take into account the elastic compression; therefore, in experimental practice, a simple linear dependence is difficult to detect at the moment of contact with a rounded indenter. According to the theory of Hertz [9], the load, F, for a ball indenter pressed against (onto) a flat plate is:

Vickers: $F = \frac{4}{3}(2.57)\,s_0^{1/2} E_{\text{eff}} s^{3/2}$,

Berkovich: $F = \frac{4}{3}(2.28)\,s_0^{1/2} E_{\text{eff}} s^{3/2}$. (10)

The radius of the ball is expressed by $R_2 \equiv 6.60\,s_0$ and $R_2 = 5.19\,s_0$ for the Vickers and Berkovich indenters, respectively.

2.3. All indenter defects, $F > F_0$, $s > s_c$

The arguments will be the same for blunted and rounded indenters and also for those with a roof edge, because the parameters in the relations for the real contact area are not essentially different, if the unrealistic maxima of tip radii are neglegted for the two indenters ($R_1 \equiv 12.7\,s_0$ for the Vickers indenter; $R_1 = 19.34\,s_0$ for the Berkovich indenter). The following principal statements can be made, assuming a homogeneous material hardness (H = constant):

a) Every case yields $\alpha_2 = 1$; therefore, the pure hardness of the bulk material will be detected by sufficiently high loads ($F \gg F_0$); this hardness, which is independent of every indenter defect, is designated as the load-independent hardness value (L_2VH) in [10]).

b) The geometry parameter α_1 can be approximated by $\alpha_1 = s_0$ for rounded indenters and by $\alpha_1 = 2\,s_0$ for blunted indenters. In practice, the indenter defect is a mixture of these two extreme cases. Therefore, one has to expect the same value for α_1 using the same indenter

for the investigation of different materials. When α_1 is estimated in this way, the value of the defect parameter, s_0, of the indenter tip can be calculated also.

c) The result of the calculation for the blunted Vickers indenter is of special interest. A good approximation yields $\alpha_0 = s_0^2$ and $\alpha_1 = 2s_0$ (see table 1); therefore, the real contact area is given by:

$$A_{\text{real}}(s) \equiv 26.43(s + s_0)^2 . \tag{11}$$

That indeed is the same expression which is used by different authors [1 and 2] to get a load-independent hardness number by addition of a constant value (here, s_0). An interpretation of this procedure is that there are systematic measurement errors of the penetration depth, s (or diagonal, d) [1 and 2]. Following this argument, the value s_0 is a correction term which can be estimated empirically by variation of the material being investigated. The term s_0 is specific for an individual indenter and must be independent of the material being investigated. The results of Ullner and Höhne [11, table 2] are in contradiction to this argument, indicating the uselessness of this s_0 correction.

3. Suppositions for an analytical study of the load dependence of the hardness given in the literature

Using equation (4) as the basis, the curve of load versus penetration depth obtained in recording hardness measurements can be analyzed by the following equation:

$$F = b_0 + b_1 s + b_2 s^2 . \tag{12}$$

The meaning of the coefficients is given by comparison with equation (4):

Vickers: $b_0 \equiv 26.43 H\alpha_0$, $b_1 \equiv 26.43 H\alpha_1$, $b_2 \equiv 26.43 H\alpha_2$;

Berkovich: $b_0 \equiv 26.98 H\alpha_0$, $b_1 \equiv 26.98 H\alpha_1$, $b_2 \equiv 26.98 H\alpha_2$.

The special equation (11) is included in equation (12) for $\alpha_0 = s_0^2$, $\alpha_1 = 2s_0$, and $\alpha_2 = 1$. The coefficient b_0 is determined by extrapolating the test results to $s = 0$ and taking b_0 as the difference between the intercept and zero on the load axis. However, using a mathematical-statistical program for correction of the zero point, this difference is smaller than the digit distance for digitally recorded measurements [5] and is, therefore, many times smaller than the critical load F_0 (i.e., $b_0 \ll F_0$). Thus, it seems legitimate to neglect the absolute term b_0 for the analysis of the loading curves and to accept the power series of Bernhardt [12] (see also [10]):

$$F_b = b_1 s + b_2 s^2 . \tag{13}$$

With $F_b = F - b_0$, the neglecting of b_0 is expressed clearly. The coefficient b_1 gives the steepness of the hardness increase in the direction of smaller loads; $b_1 = 0$ means constant hardness for an ideal indenter. The parameter b_2 is given by the product of the geometry factor and the hardness number, i.e., $b_2 = 26.43 H$.

Dividing equation (13) by $26.43 s^2$, one gets the formula for the load dependence of the Vickers hardness which is preferred over others by Knight et al. [13]:

$$H \equiv \frac{C_1}{s} + C_2 \tag{14}$$

with $C_1 = b_1/26.43$, $C_2 = b_2/26.43$. More frequently, the so-called power law of Meyer [14] is used to analyze the load dependence of hardness:

$$F = c s^n . \tag{15}$$

If $n < 2$, equation (15) gives the well-known increase of the hardness with decreasing load, with the steepness of this increase being greater for smaller exponents, n. However, it is obvious from the literature [15] that the power-law dependence can be fitted only over a small load region, at most one order of magnitude. In principle, the absence of a physical meaning of the power law in those cases where the exponent is not an integer is a strong argument against the use of Meyer's law.

4. Experimental investigations with the Berkovich indenter in the region $F < F_0$

Experiments with a Berkovich indenter on soda–lime–silica glass are chosen as a representative example to demonstrate the hardness behavior at the moment of contact. The hardness tester used was constructed as a closed-loop system. Therefore, the accumulated digital data could be used to correct the values for load and penetration depth resulting from the mathematical-statistical extrapolation of the zero point [5]. The digit distance amounts to the load detection limit of 0.4 mN. That means that the load error is smaller than 0.2 mN for these experiments [5]. A representative load/penetration curve is shown in figure 2a. Logarithmic scales are used to accentuate the situation at small loads. The monotonically increasing slope of the curve from $n = 1.02$ near $F = 0.4$ mN to $n = 1.74$ at $F = 1$ N confirms the frequently encountered experience (see section 3.) that Meyer's power law is not suitable for analyzing the load dependence of the hardness. But the plot F/s versus s with respect to equation (13) fits the experimental results very well (figure 2b). The same thing is seen in the results of Pharr et al. [16], which will be analyzed later.

The relations between load and penetration depth given in section 2. can be checked. The linearity at smallest loads at the moment of contact gives $(F/s)_{\text{exp}} = 0.06$ N/μm. The defect parameter, s_0, is calculated by

equation (6) to be ≈0.1 µm, taking E_{eff} = 70 GPa, assuming the existence of a pyramid frustum which induces elastic compression.

According to equation (5), this value of s_0 leads to a critical load F_0 = 0.3 mN, which is lower than the detection limits in these experiments. Therefore, blunting of the Berkovich indenter cannot be responsible for the linear F-s dependence at the first contact.

Assuming a rounded indenter tip, one must distinguish between elastic indentation, such as Hertzian compression, and plastic indentation, such as found in ball indentation hardness testing. The elastic deformation can be obtained using equation (10), and the plastic deformation using equation (8). Expressing these results as a ratio yields:

$$\frac{F_{plastic}}{F_{elastic}} = \frac{32.6\,H s_0 s}{3.04\,E_{eff} s_0^{1/2} s^{3/2}} = 10.7\,\frac{H}{E_{eff}} \cdot \left(\frac{s_0}{s}\right)^{1/2}.$$

With the well-known material parameters of soda–lime–silica glass ($H \approx 5$ GPa; $E_{eff} \approx 70$ GPa), one gets:

$$\frac{F_{plastic}}{F_{elastic}} = 0.764 \cdot \left(\frac{s_0}{s}\right)^{1/2}.$$

Clearly, it follows that the elastic and plastic contributions to the indentations load have the same order of magnitude, if the indentation depth, s, is nearly equal to the tip defect parameter, s_0. At $s < s_0$, the plastic deformation will dominate. Using equation (8), the value $(F/s)_{exp}$ = 0.045 N/µm leads to $s_0 \approx 0.3$ µm ($R \approx 1.6$ µm), which gives a load limit of F_0 = 0.007 N, according to equation (10). Both results agree very well with the experimental results shown in figure 2a labelled by F_0, s_c and s_0.

The influence of the real contact area of this rounded tip on the correct hardness number, $H(s)$, is shown in figure 3. Indeed, the load dependence of the hardness is partially reduced but not eliminated at small loads. It will be shown in section 5. that this result is also valid in a more general sense.

5. Investigation of the load dependence of hardness on the region $F > F_0$

A profitable way to identify the influence of tip defects of the indenter is by calculation of the ratio b_1/b_2, taking into account the regression parameters for the fitting procedure of the recorded load/penetration curves. This yields $b_1/b_2 = C_1/C_2 = \alpha_1/\alpha_2$, comparing equations (12 and 14), respectively. As was shown in section 3., one has to expect a constant value in the range $s_0 < b_1/b_2 < 2s_0$ independent of the material investigated, if the tip defects alone are responsible for the load dependence of hardness. The lower limit is due to a rounded tip and the upper limit to a blunt tip. In the following, experimental results of different authors will be tested with respect to these conditions. It will be assumed that each set of

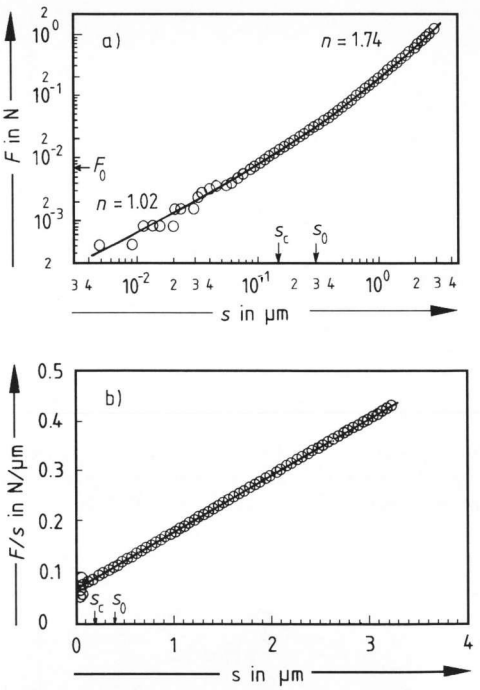

Figures 2a and b. Meyer plot (double logarithmic scales) of the load, F, versus penetration depth, s, for a Berkovich hardness measurement on soda–lime–silica glass (figure a) and analysis of the load dependence of the Berkovich hardness in a plot of F/s versus s (figure b). The full line is a fit of a linear and a power function, respectively; the 95 % confidence limit is smaller than the point diameter.

authors used the same indenter for all of its indentation experiments analyzed here. In every case, the correctness of the zero point of the accumulated load/penetration data was verified by a mathematical-statistical program [5].

Many experimental results of recording Vickers hardness measurements are known for optical glasses [17 and 18]. The regression parameters b_1 and b_2 were calculated by least-square fits based on equation (13); the results are drawn in figure 4a for flint glasses and in figure 4b for crown glasses. The expected linear correlation between the two parameters is not confirmed. Values between 0.07 and 0.55 µm were found for the ratio b_1/b_2. This difference of nearly one order of magnitude does not agree with the expected constancy of b_1/b_2.

As a second example, the results of Frischat et al. [19] were analyzed. These results were obtained with a recording Vickers microhardness tester constructed by these authors. The b_1 values must be corrected according to [5] with respect to the preload of 0.04 N used for the load sensor. The values for the calculated ratio b_1/b_2 collected in table 3 range from 0.90 to 2.28 µm. A systematic dependence on the chemical composition of the glasses could not be confirmed. A Student test was used to calculate the significance of the differences between the 78 possible combinations for the 13 glass types. With a confidence limit of 95 %, it was found that 78 % of the 78 possible combinations are significantly different.

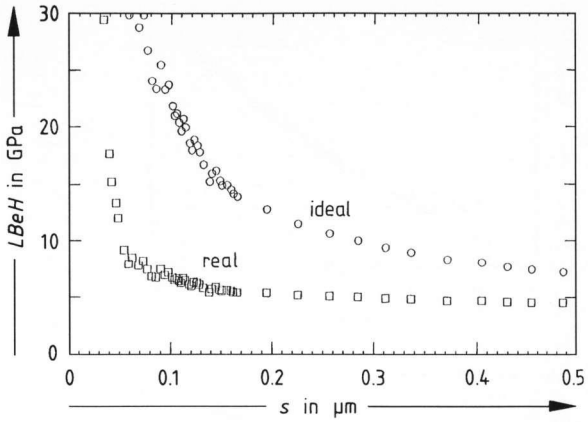

Figure 3. Load dependence of the Berkovich hardness (*LBeH*) calculated using the results of figure 2a taking the contact area of an ideal tip and a real contact area of a rounded tip.

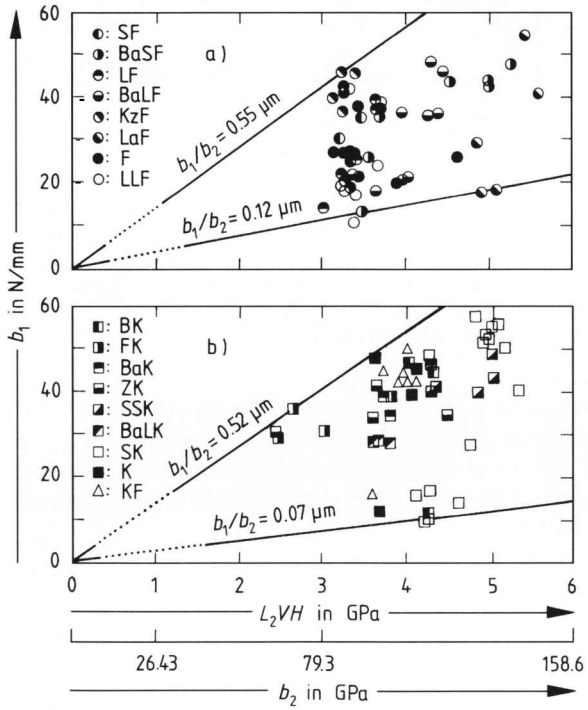

Figures 4a and b. Correlation between the parameters b_1 and b_2 of equation (13) for analysis of different glasses, a) flint glasses (Abbe number $v_e < 50$); SF = dense flint, BaSF = barium dense flint, LF = light flint, BaLF = barium light flint, KzF = short flint, LaF = lanthanum flint, F = flint, LLF = = double light flint; b) crown glasses (Abbe number $v_e > 50$); BK = borosilicate crown, FK = fluoride crown, BaK = barium crown, ZK = zinc crown, SSK = high-density crown, BaLK = barium light crown, SK = dense crown, K = crown, KF = crown flint.

Finally, results of Pharr, Oliver, and Clarke given in [16] were tested. The indentation load/displacement data were obtained with the Nanoindenter® at Oak Ridge National Laboratory using a Berkovich diamond. The results are redrawn in a plot of *F*/*s* versus *s* in figure 5 for vitreous silica at very small loads ($F < 5$ mN) and in figures 6a and b for soda–lime–silica glass and silicon single crystals ($F < 120$ mN). The parameters for linear regression are collected in table 4 and compared with

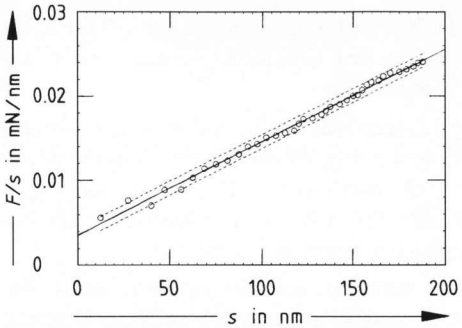

Figure 5. Plot of *F*/*s* versus *s* for analyzing the load dependence of hardness of the Nanoindenter® measurements [16] on vitreous silica. The full line is calculated by a linear fit, the dotted lines represent the 95 % confidence limit.

the experimental results of the present authors shown in figure 2b. The most important fact in this case also is the broad range of b_1/b_2 values, indicating once more the influence of material behavior and not tip defects on the load dependence of the hardness at small loads.

It is remarkable that nearly the same hardness values for soda–lime–silica glass, i.e., $L_2VH \equiv 0.03784 \cdot b_2$, were found by the three different groups of authors using different experimental conditions and working in different load regions.

6. Summary and conclusions

It is well-known that the Knoop, Vickers and Berkovich microhardness values determined in the region of ultra-low loads by measuring the diagonal of the unloaded impression or the penetration depth of the loaded impression are load-dependent. This result is unexpected in view of the self-similarity of the geometrical shape of each of these indenters.

In the present work, the influence of tip defect on the load/penetration relation was calculated and discussed in detail for blunted and rounded Vickers and Berkovich indenters. Theoretically, for loads smaller than a critical value, F_0, there should be a linear dependence on elastic contact pressure for a blunted indenter and on plastic ball indentation for a rounded indenter. Indeed, these linear relations between load and penetration depth are found experimentally for glass, but the defect parameter, s_0, arising from these results is too small to compensate for the load dependence of the hardness over the entire load scale investigated.

This result agrees very well with experiments done above the critical load F_0. It could be shown that the relation between the load, F, and the penetration depth, s, in this region can be fitted by $F = b_1 s + b_2 s^2$. If the parameter b_1, which represents the steepness of the load dependence of the hardness, is determined by the tip defect alone, then the value of the ratio b_1/b_2 must be independent of the material being investigated (for the same indenter).

Recording hardness measurements made by the present authors on many different flint and crown optical glasses show that the value of b_1/b_2 had a scatter of

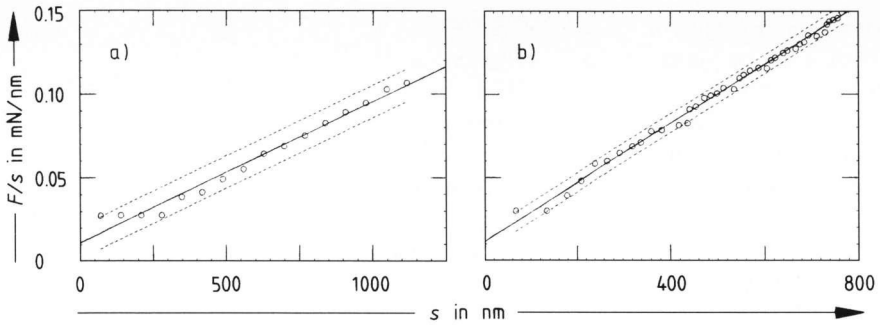

Figures 6a and b. Plot of F/s versus s for analyzing the load dependence of hardness of the Nanoindenter® measurements [16] on a) soda–lime–silica glass, b) rhombic dodecahedron (110) surfaces of silicon single crystals.

Table 3. Load independent microhardness of different glasses (from [19, tables 1 and 2])

glass no.	glass composition in mol%	b_1 [1] in N/mm	b_2 in GPa	L_2VH [2] in GPa	b_1/b_2 in µm	standard deviation in %
1	100 SiO_2	90	99.9	3.78	0.90	12.8
2	76.6 SiO_2, 13.6 Na_2O, 9.5 CaO	110	56.3	2.13	1.95	26.6
3	75 SiO_2, 25 Na_2O	95	74.5	2.82	1.27	9.7
4	75 SiO_2, 18.7 Na_2O, 6.3 Rb_2O	157	68.7	2.60	2.28	13.6
5	75 SiO_2, 12.5 Na_2O, 12.5 Rb_2O	71	60.0	2.27	1.18	9.9
6	75 SiO_2, 6.3 Na_2O, 18.7 Rb_2O	110	72.7	2.75	1.51	20.6
7	75 SiO_2, 25 Rb_2O	133	75.1	2.84	2.03	45.0
8	74 SiO_2, 17.4 Na_2O, 8.6 CaO	120	71.6	2.71	1.68	11.8
9	73.9 SiO_2, 16.2 Na_2O, 1.2 Cs_2O, 8.5 CaO	114	70.6	2.67	1.62	16.3
10	73.9 SiO_2, 13.6 Na_2O, 3.7 Cs_2O, 8.6 CaO	83	58.7	2.22	1.43	28.1
11	74 SiO_2, 9.8 Na_2O, 7.5 Cs_2O, 8.6 CaO	110	53.4	2.02	2.06	15.2
12	74 SiO_2, 6.8 Na_2O, 10.6 Cs_2O, 8.5 CaO	118	63.2	2.39	1.87	17.3
13	73.9 SiO_2, 3.6 Na_2O, 13.6 Cs_2O, 8.6 CaO	73	65.8	2.49	1.11	32.6

[1] Corrected on preload $FV \equiv 0.04\,\mathrm{N}$ [5]. [2] $L_2VH \equiv 0.03784 \cdot b_2$ [10].

Table 4. Comparison of recording hardness measurements with different load detection limits F_{lim}

test laboratory	test conditions	b_1 in N/mm	b_2 in GPa	b_1/b_2 in µm	L_2VH in GPa
Halle[3]	soda–lime–silica glass $F_{lim} \equiv 5$ mN, Vickers indenter	85.6±4.6 (5.4 %)	88.5±0.88 (1.0 %)	0.97±0.062 (6.4 %)	3.35±0.033 (1.0 %)
Freiburg[4]	soda–lime–silica glass $F_{lim} = 0.4$ mN, Berkovich indenter	66.5±0.77 (1.2 %)	86.5±0.33 (0.38 %)	0.77±0.049 (6.4 %)	3.27±0.001 (0.03 %)
Oak Ridge[5]	soda–lime–silica glass $F_{lim} \equiv 2.5$ mN, Berkovich indenter	11.11±2.23 (20.1 %)	84.2±3.3 (3.92 %)	0.132±0.032 (24.2 %)	2.94±0.115 (3.91 %)
Oak Ridge[5]	fused silica $F_{lim} = 0.1$ mN, Berkovich indenter	3.52±0.176 (5.0 %)	110.2±1.4 (1.27 %)	0.032±0.002 (6.3 %)	4.15±0.053 (1.27 %)
Oak Ridge[5]	(110) silicon single crystals, $F_{lim} = 0.1$ mN, Berkovich indenter	11.4±1.22 (10.7 %)	177.0±2.2 (1.24 %)	0.0643±0.0077 (11.9 %)	6.70±0.083 (1.24 %)

Explanation: The values in brackets stand for the deviation in %.
[3] Laboratory of the authors P. Grau, G. Berg and W. Fränzel: Fachbereich Physik, Martin-Luther-Universität, Halle (Germany).
[4] Laboratory of the author M. Schinker: Fraunhofer-Institut für Werkstoffmechanik, Freiburg (Germany).
[5] Laboratory of G. M. Pharr, W. C. Oliver and D. R. Clarke: Oak Ridge National Laboratory, Oak Ridge, TN (USA).

nearly one order of magnitude. Experimental results of Frischat et al. [19] on Na/Rb and Na/Cs silicate glasses showed that the ratio b_1/b_2 was significantly different for 78 % of the possible combinations of materials. Finally, the hardness measurements of the Nanoindenter® group at Oak Ridge [16] analyzed in this paper also led to the same conclusion for soda–lime–silica glass, vitreous silica, and silicon single crystals. Moreover, it is remarkable that this analysis of the experimental results for soda–lime–silica glass obtained by three different groups of authors in three different load regions gives essentially a single value for the parameter b_2, which is interpreted as the load-independent hardness value L_2VH in [10].

In summary, the experimental results show clearly that the load dependence of the microhardness cannot be caused solely by tip defects of the indenter. Therefore, the conclusion is that the cause of the load dependence is the material itself, responding to deformation with sharp indenters [20]. Experiments with small ball indenters are planned to test this conclusion.

*

The authors thank the Ministerium für Wissenschaft und Forschung of Sachsen-Anhalt (Germany) for sponsoring a part of this work under project no. 029A03118.

7. Nomenclature

7.1. Symbols

A	contact area in m^2
a_0	length of the square side (Vickers) or triangle side (Berkovich) of the ground faces of the blunted indenter
b_i	empirical parameter of equations (12 and 13)
C_i	empirical parameter of equation (14)
c	parameter of the Meyer law in equation (15)
d_i	diameter of indentation in mm
E	Young's modulus in Pa
F	force of the indenter in N
H	hardness number in Pa
$LBeH$	load-dependent Berkovich hardness in Pa
LVH	load-dependent Vickers hardness in Pa
m	geometrical factor in equation (6)
n	Meyer exponent in equation (15)
R	radius of the curvature of the spherical indenter defect in m
s	penetration depth in m
s_c	altitude of the ball cap
s_x	missing part of the indenter tip
s_0	defect parameter of the indenter tip in m
α_i	geometrical parameters in equation (3)
μ_i	Poisson number
v_e	Abbe number
φ, ψ	tip angles of the Berkovich indenter

7.2. Subscripts

b	Bernhardt
c	ball cap
e	green mercury line
eff	effective
exp	experimental
fic	fictive
i	index number
k	critical
lim	limit

8. References

[1] Bückle, H.: Mikrohärteprüfung und ihre Anwendung. Stuttgart: Berliner Union 1965. p. 127 ff.

[2] Mott, B. W.: Micro-indentation hardness testing. London: Butterworths 1956. p. 12, 102.

[3] Kick, F.: Das Gesetz der proportionalen Widerstände und seine Anwendungen. Leipzig: Felix 1885.

[4] Grau, P.; Berg, G.; Dengel, D.: Der Einfluß von Spitzenfehlern des Eindringkörpers auf die Prüfkraftabhängigkeit der Vickershärte. Materialprüfung **35** (1993) p. 339–342.

[5] Grau, P.: The determination of the zero point by recording microhardness tests. phys. status solidi (a). (In prep.)

[6] Weiler, W.; Behnke, H.-H.: Anforderungen an Eindringkörper für die Universalhärteprüfung. Materialprüfung **30** (1990) p. 301.

[7] Timoshenko, S.; Goodier, J. N.: Theory of elasticity. New York (et al.): McGraw-Hill 1951. p. 370.

[8] Pharr, G. M.; Oliver, W. C.; Brotzen, F. R.: On the generality of the relationship among contact stiffness, contact area and elastic modulus during indentation. J. Mater. Res. **7** (1992) p. 613–617.

[9] Hertz, H.: Über die Berührung fester elastischer Körper. J. reine angew. Math. **92** (1881) p. 156–171.

[10] Fröhlich, F.; Grau, P.; Grellmann, W.: Performance and analysis of recording microhardness tests. phys. status solidi (a) **42** (1977) p. 79–89.

[11] Ullner, C.; Höhne, L.: A critical study of recording various microhardnesses. phys. status solidi (a) **129** (1992) p. 167–180.

[12] Bernhardt, E. O.: Über die Mikrohärte der Feststoffe im Grenzbereich des Kickschen Ähnlichkeitssatzes. Z. Metallkd. **33** (1941) p. 135–144.

[13] Knight, J. C.; Page, T. F.; Hutchinson, J. M.: Surface deformation behaviour of TiN and TiC coated steels, indentation response. Surface Eng. **5** (1989) p. 213–225.

[14] Meyer, E.: Untersuchungen über Härteprüfung und Härte. Z. Ver. Dtsch. Ing. **52** (1908) no. 17, p. 645–654.

[15] Müller, B.; Grau, P.; Kluge, G.: The hardness of chromium- and titanium-doped sapphire crystals. phys. status solidi (a) **83** (1984) p. 499–504.

[16] Pharr, G. M.; Oliver, W. C.; Clarke, D. R.: Hysteresis and discontinuity in the indentation load-displacement behaviour of silicon. Scripta Metall. **23** (1989) p. 1949.

[17] Lehmann, B.: Charakterisierung der optischen Gläser mit modernen Härteprüfverfahren. Univ. Halle-Wittenberg, Dipl.-Arb. 1984.

[18] VEB Jenaer Glaswerk: Optisches Glas. Katalog. Jena 1985.

[19] Frischat, G. H.; Özmen, E.; Richter, T. et al.: Lastunabhängige Mikrohärte an verschiedenen Gläsern. Glastech. Ber. **55** (1982) no. 6, p. 119–125.

[20] Baden, M.; Dengel, D.: Vickertshärteprüfung im Kleinlast- und Mikrobereich mittels Eindringtiefemessung. Härterei-Tech. Mitt. **40** (1985) p. 107–113.

93R0949